Investigation of $L1_0$ FePt-based soft/hard composite bit-patterned media by micromagnetic simulation*

Wang Ying(王 颖)[a)†], Wei Dan(韦 丹)[b)], Cao Jiang-Wei(曹江伟)[a)], and Wei Fu-Lin(魏福林)[a)]

[a)] *Key Laboratory for Magnetism and Magnetic Materials of the Ministry of Education, Lanzhou University, Lanzhou* 730000, *China*
[b)] *Laboratory of Advanced Materials, Department of Materials Science and Engineering, Tsinghua University, Beijing* 100084, *China*

(Received 10 December 2014; revised manuscript received 9 January 2015; published online 10 April 2015)

The soft/hard composite patterned media have potential to be the next generation of magnetic recording, but the composing modes of soft and hard materials have not been investigated systematically. $L1_0$ FePt-based soft/hard composite patterned media with an anisotropic constant distribution are studied by micromagnetic simulation. Square arrays and hexagonal arrays with various pitch sizes are simulated for two composing types: the soft layer that encloses the hard dots and the soft layer that covers the whole surface. It is found that the soft material can reduce the switching fields of bits effectively for all models. Compared with the first type, the second type of models possess low switching fields, narrow switching field distributions, and high gain factors due to the introduction of inter-bit exchange coupling. Furthermore, the readout waveforms of the second type are not deteriorated by the inter-bit soft layers. Since the recording density of hexagonal arrays are higher than that of square arrays with the same center-to-center distances, the readout waveforms of hexagonal arrays are a little worse, although other simulation results are similar for these two arrays.

Keywords: micromagnetic simulation, composite bit patterned media, $L1_0$ FePt, switching field distribution, readout signal

PACS: 85.70.Ay **DOI:** 10.1088/1674-1056/24/6/068504

1. Introduction

In the research area of magnetic recording, bit-patterned media (BPM) technology[1–3] has attracted much attention in recent years since it is expected to be a promising approach to solving the contradiction between thermal stability and writability. To realize this technology, magnetic materials with high uniaxial anisotropy constant are necessary. One of the candidates is the ordered $L1_0$ phase of FePt, which possesses a very high anisotropy constant $K_u = 5 \sim 7 \times 10^7$ erg/cm^3, the unit 1 erg = 10^{-7} J.[4–7] Whereas, how to reduce its coercivity (about 110 kOe for individual bit, the unit 1 Oe = 79.5775 A·m^{-1}) to below the writing field that the magnetic head could supply (about 20 kOe)[8] is also a challenge. Composite patterned media (CPM) is a possible method to solve this problem.[9,10] This method is similar to the exchange coupled composite media (ECC media)[11–13] which have been widely investigated for improving the performances of continuous media. However, the composing mode of CPM could be different from the traditional ECC media. For CPM, soft material could enclose the hard dots and also cover the trench between recording bits. Therefore, the introduction of soft material may not only reduce the coercivity but also affect the interaction between bits. Unfortunately, the effect of soft material on the properties of $L1_0$ FePt-based CPM has not been investigated systematically. This article reports the micromagnetic simulation for two composing modes of $L1_0$ FePt-based CPM with a distribution of K_u. A commercialized micromagnetic software "LLG Micromagnetic Simulator" is adopted to create models and simulate reversal processes while a self-written program is used to simulate readout processes.

2. Simulation methods

Two types of composing are studied (Fig. 1). One is that the soft materials enclose the hard dots only (A-type), the other is that the soft materials cover the whole surface of the medium (B-type). Traditionally, the array of recording units for BPM is square, but the hexagonal array is also applicable since this type of media with good dimensional uniformity and narrow switching field distribution can be fabricated by block copolymer directed assembly.[14,15] Thus, both the square array and hexagonal array are simulated for each type.

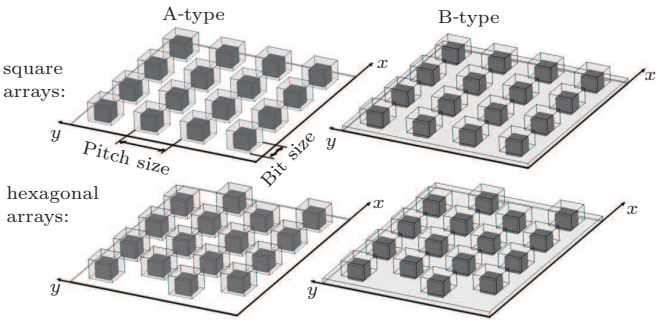


Fig. 1. Models of simulation. Dark parts and grey parts are hard materials and soft materials, respectively.

*Project supported by the National Natural Science Foundation of China (Grant Nos. 51171086 and 61272076) and the Young Scientists Fund of the National Natural Science Foundation of China (Grant No. 61003041).

†Corresponding author. E-mail: yingw@lzu.edu.cn

© 2015 Chinese Physical Society and IOP Publishing Ltd

Table 1. Pitch sizes and recording densities of models. The unit 1 in = 2.54 cm.

	Square array			Hexagonal array		
Pitch size in x direction/nm	16	20	24	16	20	24
Pitch size in y direction/nm	16	20	24	14	18	20
Recording density/(Tbit/in^2)	2.5	1.6	1.1	2.9	1.8	1.3

We consider arrays of 4×4 bits for all models. Each bit has a total size of 12 nm×12 nm×8 nm in which the hard dot is 8 nm×8 nm×6 nm and soft layer has a thickness of 2 nm. For B-type models there is also a 2-nm-thick soft layer between bits. Pitch sizes and corresponding recording densities are listed in Table 1. The pitch sizes of the y direction for hexagonal arrays are smaller since the center-to-center distances should be the same. The size of the micromagnetic cells was set to be 2 nm×2 nm×2 nm. The saturation magnetization (M_s) of soft layer is 1900 emu/cm^3, which is the highest value of FeCo alloy. The magnetocrystalline anisotropy of the soft layer is ignored. For hard dots, the magnetic parameters of $L1_0$ FePt are adopted: the M_s is 1140 emu/cm^3; the uniaxial perpendicular anisotropy constant K_u is 5×10^7 erg/cm$^{-3} \sim 7 \times 10^7$ erg/cm^3. Due to the astriction of bit number, the K_u of hard dots follows a simple distribution as shown in Fig. 2 and is randomly assigned. The exchange coupling constants for soft and hard parts and between soft and hard parts were all set to be 1×10^{-6} erg/cm. External field is in the direction parallel to the easy axis of bits. To avoid numerical instabilities, the initial magnetic moment directions of all cells have a 3°-angle with respect to the perpendicular direction. Since we focus on the switching fields of recording bits, only the descending branches of hysteresis loops are simulated.

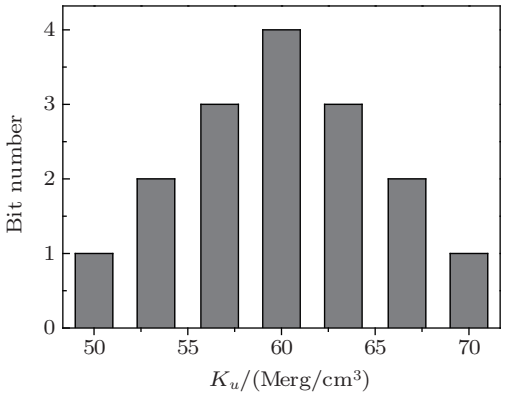


Fig. 2. Distribution of K_u for the hard parts of bits in simulation.

The readout waveforms of the media of different types are also simulated. For each type, a new model with 3 tracks along the x direction and 12 dots for each track are established. A giant magnetoresistive (GMR) reading head model with a shield-to-shield separation of 6 nm, sensor width of 12 nm, and sensor length of 3 nm is adopted to replay the signal.

3. Results and discussion

Figure 3 shows the simulation results of square and hexagonal arrays for A-type models. The curves of the two arrays are similar. At the beginning the magnetizations of all models keep constant, and then decrease when the external field reaches the switching fields of the bits with the weakest anisotropy. After the reversal of the bits with the highest anisotropy, the magnetization becomes constant again. Due to the limited number of bits, all of the curves show steps in decreasing processes, which correspond to the individual reversal of bits. These curves indicate that the exchange coupling between soft and hard materials is strong enough to ensure the coherent reversal of one bit. On the other hand, the slopes of the decreasing parts of curves increase with increasing pitch size. For analyzing precisely, the switching field of every bit is recorded. The results are shown in Fig. 4. Compared with the individual composite bits, the in-array-bits with small anisotropy constants (below 6×10^7 emu/cm^3), which also reverse earlier, have smaller switching fields. Oppositely, the bits with high anisotropy constants (above 6×10^7 emu/cm^3) have higher switching fields than the individual bits. With the decrease of pitch size, the differences in switching field between individual bits and in-array-bits become more obvious. These phenomena are all consistent with the characteristics of magnetostatic interaction.

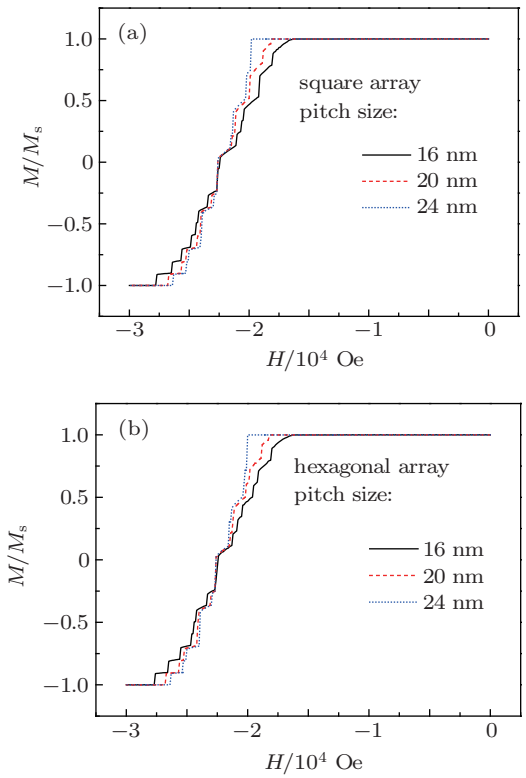


Fig. 3. (color online) Descending branches of hysteresis loops for A-type models.

Simulation results of B-type models are shown in Fig. 5. For the models with a pitch size of 16 nm, the magnetization

keeps constant at the beginning, and then decreases slowly as the external field increases. The decrease corresponds to the tilt of the magnetic moment of the inter-bit soft layer. These soft cells have weak exchange coupling with hard dots, so their magnetic moments cannot keep the perpendicular state under the joint action of the external field and demagnetizing field. When the pitch size increases to 20 nm and 24 nm, the exchange coupling between these soft cells and hard dots is so weak that the magnetic moments of these soft cells become declining even the external field is zero. Meanwhile, the area of the inter-bit soft layer increases with increasing pitch size, so the total magnetization of the model with larger pitch size decreases more distinctly before the reversal of bits. For these models the reversal of bits also leads to the steps of curves. Figure 6 shows the switching fields of bits. The switching fields of bits for B-type models are about one quarter lower than those of the individual composite bits with the same anisotropy constant. Most of the bits have lower switching fields than the writing field of magnetic head (20 kOe). The larger the pitch size, the lower the switching fields are. This result may come from the fact that the inter-bit soft layers also help to reduce the switching fields. When the pitch size increases from 16 nm to 20 nm, the decrease of switching fields is obvious. However, the further increase of pitch size could not reduce the switching fields very much. It can be deduced that only the soft cells close to bits (the distance is less than 4 nm) could affect the switching fields of bits obviously.

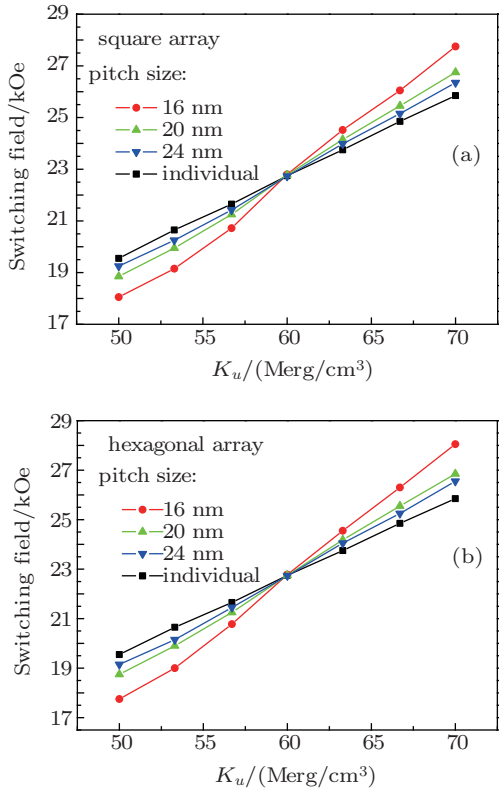


Fig. 4. (color online) Switching fields of bits with various values of K_u for A-type models. For the bits with the same K_u, the values are averaged.

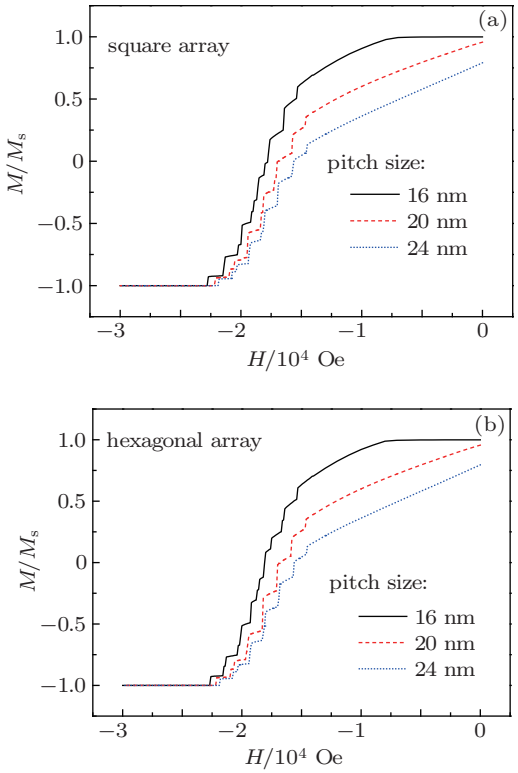


Fig. 5. (color online) Descending branches of hysteresis loops for B-type models.

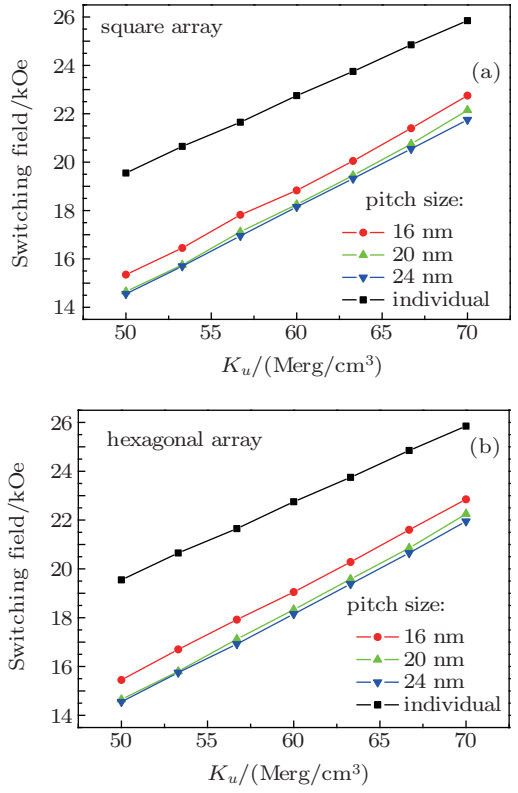


Fig. 6. (color online) Switching fields of bits with various values of K_u for B-type models. For the bits with the same K_u, the values are averaged.

Normally the value of switching field distribution (SFD), which could be obtained by fitting the derivative of reversal curves using certain equations, can reflect the interaction be-

tween recording bits. However, in our simulation the SFD values are hard to calculate due to the limit of bit number. So we define a parameter $\Delta H = H_{\max} - H_{\min}$, where $H_{\max}$ and $H_{\min}$ are the maximal and minimal switching fields of bits, respectively, to signify the range of switching fields. The values of ΔH for all simulated models are shown in Fig. 7. It can be observed that the values of ΔH for all models are almost the same when the pitch size is 24 nm. With the decrease of pitch size, ΔH increases significantly for A-type models, whereas it does not change very much for B-type models. It is easy to understand that the increase of ΔH for A-type models is caused by strengthening the magnetostatic interactions. However, for B-type models the exchange coupling interactions between bits also exist due to the inter-bit soft layers. On the contrary to the magnetostatic interaction which forces two dipoles to aline antiparallelly, the exchange coupling interaction makes dipoles point to the same direction, so that ΔH will be reduced. Figure 8 shows the magnetostatic energy and exchange energy of one bit obtained from other bits and the soft layer. The magnetostatic energy is calculated when all bits point to the same direction, while the calculation of the exchange energy is a little complex since the exchange interaction between bits is not direct but through the soft layer. In this investigation the exchange energy of one bit obtained from other bits is defined as the difference value in exchange energy between two states: other bits point to the same direction as or to the one opposite to the chosen one. It can be observed that when the pitch size is 24 nm, the exchange coupling interactions between bits of B-type models are very weak so their ΔH values are mainly affected by magnetostatic interactions which is the same as those of A-type models. With the decrease of pitch size, the two interactions increase simultaneously. Since the exchange coupling interaction counteracts the magnetostatic interaction, the ΔH values of B-type models remain unchanged. Whereas, the ΔH values of B-type models are all larger than those of the individual bits. That means that the magnetostatic interactions are still the main interactions. It is noticed that although the exchange energy is much smaller than the magnetostatic energy, it still has a very obvious influence on switching field and ΔH.

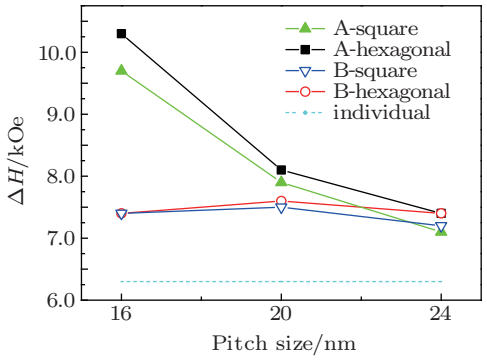


Fig. 7. (color online) Values of ΔH of all models versus pitch size.

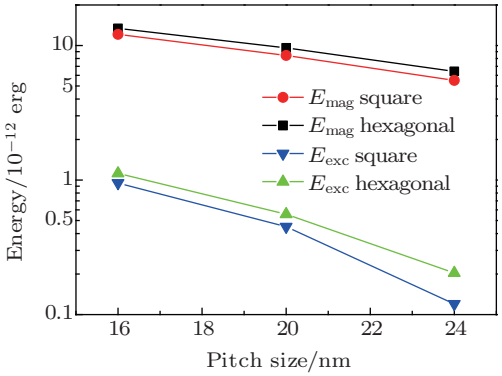


Fig. 8. (color online) Variations of magnetostatic energy ($E_{\rm mag}$) and exchange energy ($E_{\rm exc}$) of one bit obtained from other parts of B-type medium with pitch size.

Under the same pitch size, the recording density of a hexagonal array is about 1.15 times that of a square array. However, the differences in switching field and switching field distribution between square and hexagonal arrays with the same pitch size are not found in our simulations very much. For A-type models, the coercivities of the two arrays are the same, but the ΔH of hexagonal arrays are a little larger than those of square arrays with the same pitch size. This is because the hexagonal arrays possess higher densities of bits and stronger magnetostatic interactions. Whereas for B-type models, the switching fields of hexagonal arrays are a little higher than or equal to those of square arrays since the hexagonal arrays are of less inter-bit soft materials. When the pitch size is 24 nm, the ΔH of the hexagonal array is larger than that of the square array. This result is the same as that from the A-type models and is also caused by stronger magnetostatic interaction of the hexagonal array as shown in Fig. 8. With the decrease of pitch size, the ΔH values of two types of arrays become closer. Although the exchange coupling and magnetostatic interactions both increase with decreasing pitch size, the exchange coupling interaction of hexagonal arrays increases more obviously (increases by 0.92×10^{-12} erg for hexagonal arrays and 0.83×10^{-12} erg for square arrays) so that the counteraction to magnetostatic interaction is stronger and the ΔH becomes smaller.

The gain factor ξ is important for ECC media since it reflects the improvement in thermal stability compared with the single layer media. It is defined as:[8]

$$\xi = \frac{2\Delta E}{H_{\rm sw} M_{\rm s} V}, \tag{1}$$

where ΔE is the uniaxial anisotropic energy, which is also the energy barrier for the thermal reversal of magnetic moment. $M_{\rm s}$ and V are the average $M_{\rm s}$ and total volume of particle, respectively. To determine the ξ of our model, the energy barrier ΔE for the thermal reversal of recording bits should be calculated first. It is easy to calculate the values of ΔE of the A-type

models because their recording bits are separated so that the magnetocrytalline energy and demagnetic energy of a single bit determine the ΔE. Whereas for B-type models, the recording bits are connected by soft material, so it is a little difficult to figure out ΔE. To simplify the problem, we consider the demagnetized case. That is, the numbers of bits whose magnetic moments point up and down are the same. In that case, for one bit the exchange energy and magnetostatic energy from other bits can be neglected since these energies from different bits are offset by each other. Besides, it is also necessary to find out the region of thermal reversal. Figure 9 shows that only the soft layer which attaches to the hard core could keep a similar moment direction to the hard part. Therefore, the values of ΔE of B-type models are the same as those of A-type models. The values of ξ for all models are listed in Table 2. It can be observed that the values of ξ of A-type models are very close to 1. That means that there is no benefit of thermal stability for A-type models compared with single material BPM due to strong exchange coupling between soft and hard parts. However, for B-type models the thermal stability can be improved by about 30% since the inter-bit soft layers are conducible to the reversal of bits in applied magnetic field but have no contribution to thermal reversal.

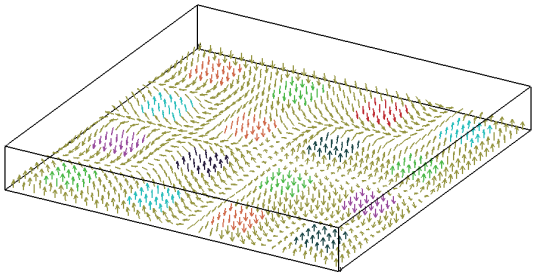


Fig. 9. (color online) Magnetic moment state for the bottom layer of a square B-type model with a pitch size of 16 nm in zero field. Half the bits are set to be reversed.

Table 2. Values of gain factor ξ for all models.

	Square array			Hexagonal array		
Pitch size/nm	16	20	24	16	20	24
for A-type models	1.02	1.02	1.02	1.02	1.02	1.02
for B-type models	1.23	1.28	1.28	1.22	1.27	1.28

The readout waveforms of the media of different types are shown in Fig. 10. The signal of the middle track is set to be 010011010011 (0: moment is down; 1: moment is up) and the two side tracks are set to be opposite in direction. It can be observed that the waveforms of A-type and B-type are very similar. The inter-bit soft layer seems to have very little interference on the replay signal. Compared with the waveforms of the media of square arrays, the results of hexagonal arrays possess less distinctive transitions of peaks, especially for the ones with the pitch size of 16 nm. According to the investigation by Nutter *et al.*[16] the readout performances of hexagonal arrays should be better than those of square arrays if their track separations are the same. Whereas in our research, this phenomenon is not observed since the track separations of hexagonal arrays are set to be smaller than those of square arrays.

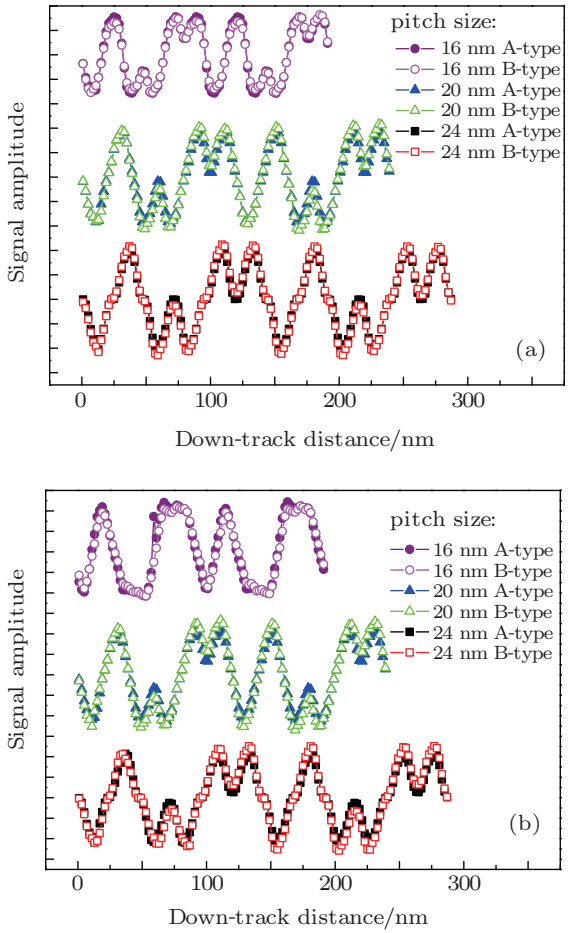


Fig. 10. (color online) Readout waveforms for the media of two types: (a) square array, (b) hexagonal array.

4. Conclusions

Two composing types and two arrays of $L1_0$ FePt-based CPM are studied by micromagnetic simulation. As a comparison between the two composing types, the B-type in which the soft material covers the whole surface of media can reduce the switching fields of bits more effectively. Due to the exchange coupling interactions induced by inter-bit soft layer, the switching field distributions of B-type models are smaller and change little with the variation of pitch size. In addition, the inter-bit soft layer of B-type models could help to improve the gain factor but does not affect the readout signals obviously. For the square and hexagonal arrays with the same center-to-center distance, the simulation results of magnetic reversal are similar although the recording densities of hexagonal arrays are higher. However, the readout performance of the hexagonal array is not as good as that of the square array with the same pitch size due to the smaller track distance.

References

[1] Chou S Y, Wei M, Krauss P R and Fischer P B 1994 *J. Vac. Sci. Technol. B* **12** 3695

[2] White R L, New R M H and Pease R F W 1997 *IEEE Trans. Magn.* **33** 990

[3] Weller D and Moser A 1999 *IEEE Trans. Magn.* **35** 4423

[4] Usov N A and Barandiarán J M 2012 *Appl. Phys. Lett.* **101** 172402

[5] Jia Y F, Shu X L, Xie Y and Chen Z Y 2014 *Chin. Phys. B* **23** 076105

[6] Liu L W, Dang H G Sheng W, Wang Y, Cao J W, Bai J M and Wei F L 2013 *Chin. Phys. B* **22** 047503

[7] Liu X and Ishio S 2013 *Chin. Phys. B* **22** 087504

[8] Batra S, Hannay J D, Hong Z and Goldberg J S 2004 *IEEE Trans. Magn.* **40** 319

[9] Goh C K, Yuan Z M and Liu B 2009 *J. Appl. Phys.* **105** 083920

[10] Krone P, Makarov D, Schrefl T and Albrecht M 2010 *Appl. Phys. Lett.* **97** 082501

[11] Wang Y, Wang R, Xie H L, Bai J M and Wei F L 2013 *Chin. Phys. B* **22** 068506

[12] Victora R H and Shen X 2005 *IEEE Trans. Magn.* **41** 537

[13] Wang J P, Shen W K, Bai J M, Victora R H, Judy J H and Song W L 2005 *Appl. Phys. Lett.* **86** 142504

[14] Ruiz R, Kang H, Detcheverry F A, Dobisz E, Kercher D S, Albrecht T R, de Pablo J J and Nealey P F 2008 *Science* **321** 936

[15] Hellwig O, Bosworth J K, Dobisz E, Kercher D, Hauet T, Zeltzer G, Risner-Jamtgaard J D, Yaney D and Ruiz R 2010 *Appl. Phys. Lett.* **96** 052511

[16] Nutter P W, Ntokas I T, Middleton B K and Wilton D T 2005 *IEEE Trans. Magn.* **41** 3214